Localization of growth sites in diffusion-limited-aggregation clusters: Multifractality and multiscaling

Jysoo Lee
Center for Polymer Studies and Department of Physics, Boston University, Boston, Massachusetts 02215 and Höchstleistungsrechenzentrum, Kernforschungsanlage Jülich, Postfach 1913, W-5170 Jülich, Germany

Stefan Schwarzer
Center for Polymer Studies and Department of Physics, Boston University, Boston, Massachusetts 02215

Antonio Coniglio
Center for Polymer Studies and Department of Physics, Boston University, Boston, Massachusetts 02215 and Dipartimento di Scienze Fisiche, Universita degli Studi di Napoli, I-80125 Napoli, Italy

H. Eugene Stanley
Center for Polymer Studies and Department of Physics, Boston University, Boston, Massachusetts 02215
(Received 12 April 1993)

The growth of a diffusion-limited-aggregation (DLA) cluster with mass M and radius of gyration R is described by a set of growth probabilities $\{p_i\}$, where p_i is the probability that the perimeter site i will be the next to grow. We introduce the joint distribution $N(\alpha, x, M)$, where $N(\alpha, x, M)d\alpha dx$ is the number of perimeter sites with α values in the range $\alpha \le \alpha_i \le \alpha + d\alpha$ (α sites) and located in the annulus $x \le x_i \le x + dx$ around the cluster seed. Here, $\alpha_i \equiv -\ln p_i / \ln R$ if $p_i > 0$, $x_i \equiv r_i/R$, and r_i is the distance of site i from the seed of the DLA cluster. We use $N(\alpha, x, M)$ to relate multifractal and multiscaling properties of DLA. In particular, we find that for large M the location of the α sites is peaked around a fixed value $\bar{x}(\alpha)$; in contrast, the perimeter sites with $p_i = 0$ are uniformly distributed over the DLA cluster.

PACS number(s): 68.70.+w, 61.43.Hv, 05.40.+j, 81.10.−h

I. INTRODUCTION

The growth of a diffusion-limited-aggregation (DLA) [1–14] cluster with mass M is described by the set of growth probabilities $\{p_i\}$ [15–18] where p_i is the probability that perimeter site i will be the next to grow. One way to analyze the set $\{p_i\}$ is by calculating the "growth-probability distribution" $n(\alpha, M)$, where $n(\alpha, M)d\alpha$ is the number of perimeter sites with $\alpha \le \alpha_i \le \alpha + d\alpha$,

$$\alpha_i \equiv -\ln p_i / \ln R, \tag{1}$$

and R is the radius of gyration of the cluster [18,19]. We call α sites those sites which are characterized by the same value of α. The main motivation for studying the distribution $n(\alpha, M)$ is its relation to the multifractal spectrum $f(\alpha)$ [17,18,20,21] of the "measure" $\{p_i\}$. We define $f(\alpha, M)$ through

$$n(\alpha, M) \equiv M^{\nu f(\alpha, M)}, \tag{2}$$

where ν is the inverse fractal dimension of DLA, $R \sim M^{\nu}$. If for large M $f(\alpha, M)$ converges to an M-independent function $f(\alpha)$, then $f(\alpha)$ is usually called the multifractal spectrum. For two-dimensional (2D) DLA, there exist several studies [22–24] proposing different convergence behaviors and functional forms of $f(\alpha)$ in the limit $M \to \infty$. However, these considerations will not be essential for our arguments concerning the relation of multiscaling and multifractality. Henceforth we will only assume that some $f(\alpha)$ exists.

During the process of calculating $n(\alpha, M)$, the information about the location of the α sites is lost. However, some information about the location of the growth sites and their associated values p_i may be obtained from the Plischke-Rácz probability $P(x, M)$ [25], where $P(x, M)dx$ is the probability that the next particle will be deposited at a rescaled distance $x \le x_i \le x + dx$. Here $x_i \equiv r_i/R$ and r_i is the distance from the cluster seed. For DLA, the function $P(x, M)$ displays a peak at a constant value $\bar{x}$ of the deposition radius [25].

A simple form for $P(x, M)$ is the Gaussian function

$$P(x, M) = \frac{1}{\sqrt{2\pi\xi^2}} \exp\left[-\frac{(x - \bar{x})^2}{2\xi^2}\right], \tag{3}$$

where ξ^2 denotes the mean-square width of the deposition zone. Plischke and Rácz (PR) [25] suggest that $\xi \sim M^{\nu' - \nu}$, $\nu' < \nu$, where ν is the inverse fractal dimension of DLA, $R \sim M^{\nu}$, and ν' an independent exponent. However, Meakin and Sander [26] find that ν' approaches ν as M increases. They also argue that $\nu = \nu'$ in the limit $M \to \infty$.

If $(\bar{x}/\xi)^2 \simeq 2c \ln M$ [27] with constant c, then $P(x, M)$ takes the form

$$P(x, M) = \frac{1}{\sqrt{2\pi\xi^2}} M^{-\phi(x)} C_{\mathrm{PR}}(x), \tag{4}$$

where from (3) $\phi(x) = c(x/\bar{x} - 1)^2$ and $C_{\mathrm{PR}}(x) = 1$. In

general, if $C_{\rm PR}(x)$ is a generic function of x and $\phi(x)$ is independent of x we have conventional scaling while if $\phi(x)$ is x dependent we say that we have *multiscaling.*

Next, we introduce the annular density $\rho_A(x,M)$, where $\rho_A(x,M)dx$ is the number of particles in an annulus $[x,x+dx]$ and related to the conventional particle density $\rho(r,M)$ by $\rho_A(x,M)dx = 2\pi r\rho(r,M)dr$. Since the change of $\rho_A(x,M)$ with increasing cluster mass is given by $P(x,M)$ [25], i.e.,

$$\frac{\partial}{\partial M}\rho_A(x,M) = P(x,M), \tag{5}$$

it was suggested [28] to write $\rho_A(x,M)$ in the same multiscaling form as Eq. (4),

$$\rho_A(x,M) = r^{D(x)}C_\rho(x), \tag{6}$$

where $D(x)$ is the fractal dimension for a thin annulus with average radius x and $C_\rho(x)$ is an amplitude. Note that if $\phi = \phi(x)$ in Eq. (4), then also $D = D(x)$ in (6). Multiscaling in (6) has been supported by simulations [28]. Whereas multiscaling for clusters with $M < 10^6$ has been confirmed very recently by Ossadnik [29], the same study analyzes one very large off-lattice cluster of $M = 5\times 10^7$ arriving at an ambiguous result, which is consistent with both multiscaling and standard scaling of $\rho_A(x,M)$.

As demonstrated in Ref. [27], multiscaling results if the α sites are "localized" in space. Here, we study the nature of the "localization" of the α sites and the nonlocalized behavior of the $p_i = 0$ ("dead") perimeter sites (Secs. II and III). The consequences for the multiscaling hypothesis of $P(x,M)$ and $\rho_A(x,M)$ will be discussed in Sec. IV. Moreover, we introduce the notion of a multifractal spectrum in an annulus and find an intriguing combination of multifractal and multiscaling properties (Sec. V) [30].

II. THE JOINT DISTRIBUTION FUNCTION

In this section we introduce the joint distribution function $N(\alpha,x,M)$, where $N(\alpha,x,M)d\alpha dx$ is the number of perimeter sites with $p_i > 0$ such that $\alpha \le \alpha_i \le \alpha + d\alpha$ and within the annulus $[x,x+dx]$. The distribution $N(\alpha,x,M)$ can be related to the three functions discussed in the introduction.

(a) $n(\alpha,M)$. By integration of $N(\alpha,x,M)$ over x, we have

$$n(\alpha,M) = \int dx\, N(\alpha,x,M). \tag{7}$$

(b) $P(x,M)$. If we use Eq. (1) together with the relation $R = M^\nu$ — which reflects the well-established fractal structure of DLA — to write the growth probability as $M^{-\nu\alpha}$, then

$$P(x,M) = \int d\alpha\, N(\alpha,x,M)M^{-\nu\alpha}. \tag{8}$$

(c) $\rho_A(x,M)$. One possibility to express $\rho_A(x,M)$ in terms of $N(\alpha,x,M)$ is by using Eqs. (5) and (8). Integration of Eq. (5) with respect to M yields

$$\rho_A(x,M) = \int_1^M dM' \int d\alpha\, N(\alpha,x,M')(M')^{-\nu\alpha}. \tag{9a}$$

However, we would like to point out another relationship that does not involve an integration over the growth history of the cluster. First, note that $N(\alpha,x,M)$ only describes perimeter sites with growth probability $p_i > 0$ (alive perimeter sites — in contrast to dead sites with $p_i = 0$; see Fig. 1). We denote the annular density profile of alive perimeter sites by $\rho_A^{(a)}(x,M)$ and that of dead perimeter sites by $\rho_A^{(d)}(x,M)$, both defined in analogy to $\rho_A(x,M)$, which describes the density of cluster sites. The sum $\rho_A^{(a)}(x,M) + \rho_A^{(d)}(x,M)$ describes *all* perimeter sites of clusters of mass M. Since DLA is a treelike fractal object [31], we expect the annular density of all perimeter sites to be proportional to the annular density of cluster sites $\rho_A(x,M)$. Furthermore, as one can see from Figs. 2 and 3, the spatial distributions of dead and alive sites are in good approximation proportional to each other, i.e., $\rho_A^{(a)}(x,M) \sim \rho_A^{(d)}(x,M)$; a detailed discussion is given in Appendix A. Consequently, we expect

$$\rho_A(x,M) \sim \int d\alpha\, N(\alpha,x,M). \tag{9b}$$

III. SIMULATION APPROACH

A calculation of the joint distribution $N(\alpha,x,M)$ shows that the x dependence is approximately Gaussian, centered around a value $\bar{x} \equiv \langle x\rangle$ with variance $\xi^2(\alpha,M) \equiv \langle x^2\rangle - \langle x\rangle^2$, i.e.,

$$N(\alpha,x,M) \propto \frac{1}{\sqrt{2\pi\xi^2(\alpha,M)}}\exp\left[-\frac{[x-\bar{x}(\alpha)]^2}{2\xi^2(\alpha,M)}\right]. \tag{10}$$

Here, the brackets $\langle\ \rangle$ indicate an expectation value with respect to the empirical distribution $N(\alpha,x,M)$, i.e., $\langle f(x)\rangle \equiv \int dx f(x)N(\alpha,x,M)/\int dx N(\alpha,x,M)$.

In Fig. 4, we show $N(\alpha,x,M)$ with $M = 20\,000$ for α values of 1.1, 1.5, 1.9, 2.3, and 2.8 vs $\pm(x-\bar{x})^2$, where

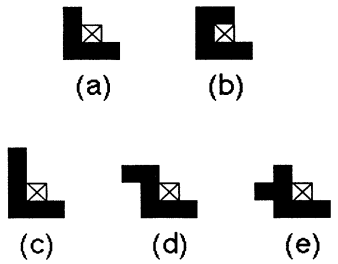

FIG. 1. (a) The lowest-order configuration which contains a dead site (×). (b)–(e) Examples of higher-order configurations containing dead sites.

the + sign applies if $x \geq \bar{x}$ and − otherwise. The Gaussian approximation (10) is justified, since we observe for positive and negative abscissa values an approximate straight-line behavior of $N(\alpha, x, M)$. For each α, the modulus of the slope $m(\alpha)$ of these lines relates to the width of the Gaussian function, $|m(\alpha)| = 1/2\xi^2(\alpha, M)$. Apparently, $\xi(\alpha, M)$ increases with α. In other words, highly screened growth sites are less localized than the exposed growth sites in the active region of the cluster that are characterized by small values of α. The approximation is worse for $x < \bar{x}$, where especially for large values of α the presence of the cluster center distorts the pure Gaussian behavior [34].

In Fig. 5 we demonstrate that α sites are located in approximate annuli around the center of the cluster by

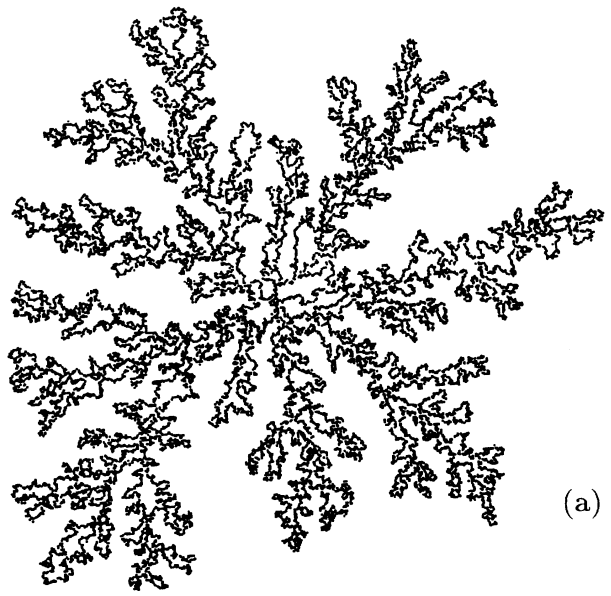

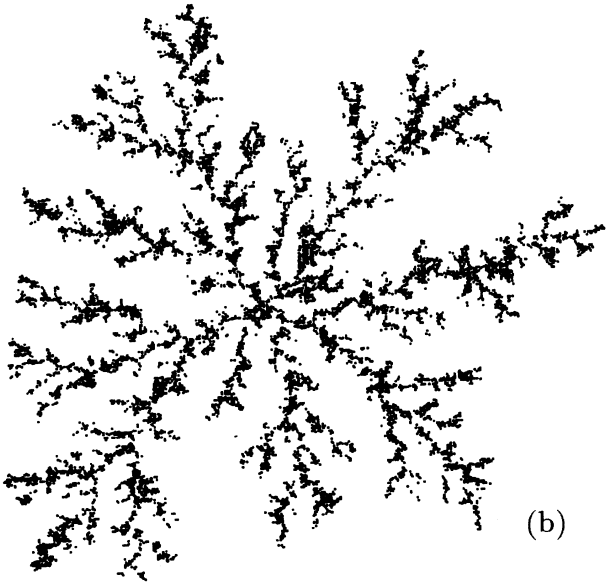

FIG. 2. (a) Dead and (b) alive growth sites of a DLA cluster with $M = 20\,000$, indicating the similar spatial distribution of both types of perimeter sites. Dead sites are perimeter sites with $p_i = 0$. Reference [19] finds that the number of dead perimeter sites in DLA is proportional to the number of all perimeter sites. In our case, dead sites constitute a fraction of $\approx 42\%$ of the perimeter sites.

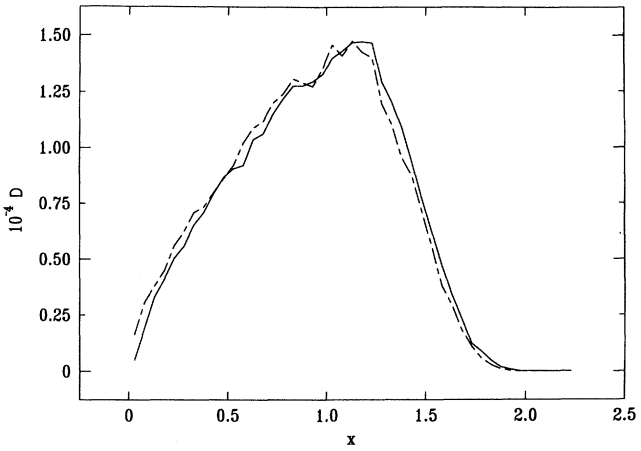

FIG. 3. Comparison of the two distributions $\mathcal{D}$ of dead sites, $\rho_A^{(d)}(x, M)$ (broken line), and of alive sites, $\rho_A^{(\alpha)}(x, M)$ (solid line). To demonstrate that both are distributed in a similar fashion, we have scaled $\rho_A^{(d)}(x, M)$ by the ratio of the number of alive to dead perimeter sites (= 1.36).

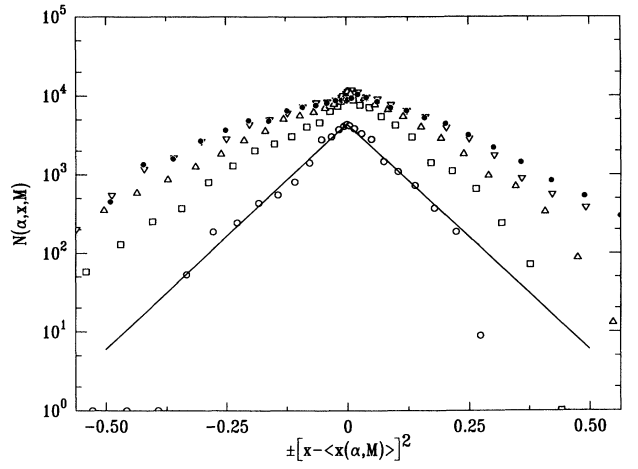

FIG. 4. $N(\alpha, x, M)$ averaged over 18 clusters of mass $M = 20\,000$. Different symbols denote different values of α: 1.1 (○), 1.5 (□), 1.9 (△), 2.3 (▽), and 2.8 (•). To test whether the x dependence of $N(\alpha, x, M)$ can be represented by a Gaussian function, we plot $\pm(x - \langle x \rangle)^2$ on the abscissa, where the + sign applies if $x \geq \langle x \rangle$ and the − sign otherwise. The ordinate scale is logarithmic. Thus Gaussian behavior manifests itself in two straight lines emanating from $x - \langle x \rangle = 0$ with slopes of opposite sign but equal magnitude. The two solid lines in the plot illustrate this behavior and are intended as guides to the eye for the case $\alpha = 1.1$.

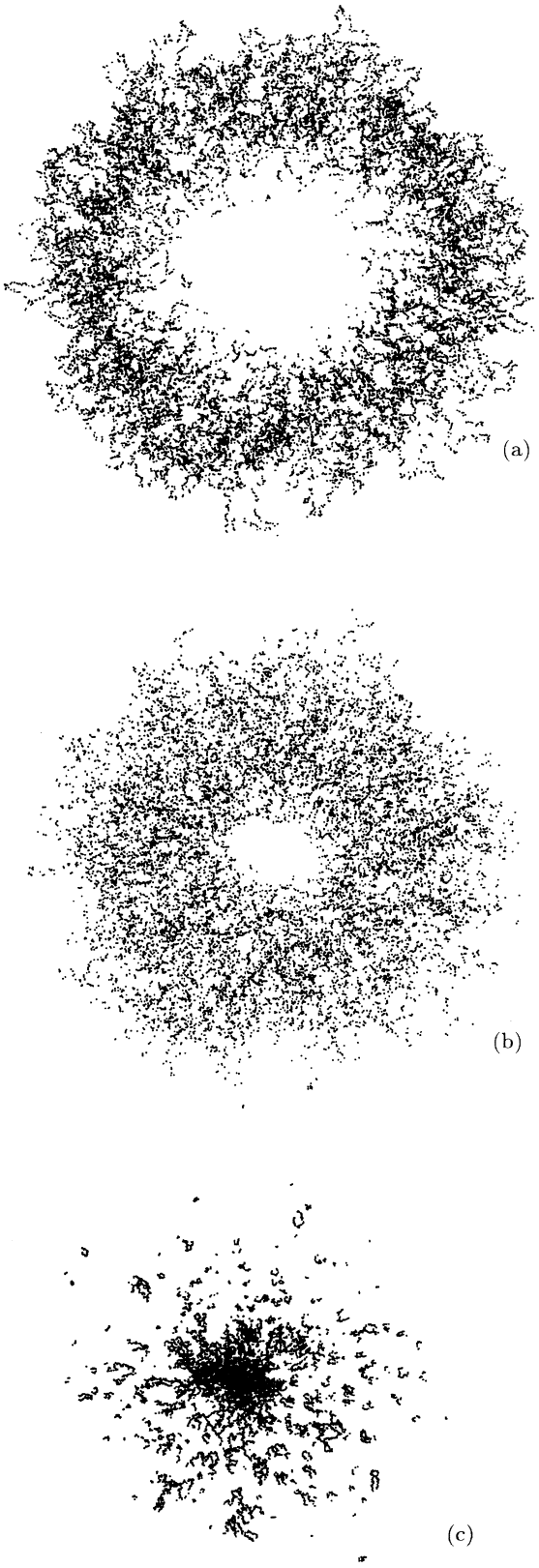

FIG. 5. Location of α sites from 18 off-lattice DLA clusters of $M = 20\ 000$. In (a) we have $1.5 < \alpha < 1.9$, in (b) $2.8 < \alpha < 3.0$, and in (c) $\alpha > 6$.

displaying all the "live" ($p_i > 0$) perimeter sites of 18 superposed off-lattice DLA clusters of $M = 20\ 000$ for three distinct values of α. In contrast, the dead sites of a cluster, as shown in Fig. 2a, are distributed with a density proportional to that of the alive sites (cf. Appendix A), which, for comparison, are displayed in Fig. 2b.

The M dependence of the width $\xi(\alpha, M)$ is shown in Fig. 6(a). We cannot identify an unequivocal limit behavior as a function of M. For certain values of α, $\xi(\alpha, M)$ seems to decrease as $M \to \infty$ — for others an increase is observed. The best statistics are obtained for $\alpha \approx 1.36$, for which we find a decreasing width. Since asymptotically $\xi(\alpha, M)$ can certainly not increase — which would correspond to the statement that the growth zone would become larger than the cluster itself — we are clearly still in a mass regime where finite-size effects play an important role. Thus, we will have to discuss several possibilities for the M dependence of $\xi(\alpha, M)$ in the following sections.

The M dependence of the mean $\bar{x}(\alpha, M)$ is plotted in Fig. 6(b). Unlike in the case of the width $\xi(\alpha, M)$, here the limit behavior for large M is manifest. For small values of α, $\bar{x}(\alpha, M)$ decreases with M while for large α, $\bar{x}(\alpha, M)$ increases with M. However, in both cases $\bar{x}(\alpha, x, M)$ converges towards an M-independent limit $\bar{x}(\alpha)$, as shown in Fig. 6(c). Note that $\bar{x}(\alpha)$ is a monotonically decreasing function and thus invertible. The decrease of $\bar{x}(\alpha)$ with α results from the stronger screening (large α) in the interior of the cluster (small x).

IV. MULTISCALING OF $P(x, M)$ AND $\rho_A(x, M)$

Next we discuss the functional form of the new distribution function $N(\alpha, x, M)$. As we have shown above, our calculations are consistent with the possibility that for large M, $N(\alpha, x, M)$ is a Gaussian function [32] in x,

$$N(\alpha, x, M) = \frac{M^{\nu f(\alpha)}}{\sqrt{2\pi\xi^2(\alpha, M)}} \exp\left[-\frac{[x - \bar{x}(\alpha)]^2}{2\xi^2(\alpha, M)}\right]. \quad (11)$$

In (11) we write $\bar{x} = x(\alpha)$, since we have found that $\bar{x}$ for large M depends only on α. The term $M^{\nu f(\alpha)}$ in the prefactor of the Gaussian ensures that $n(\alpha, M)$ has the multifractal form (2), as one can see by integration with respect to x.

We next discuss the implications for multiscaling of several possibilities for the functional dependence of the width $\xi(\alpha, M)$ on α and M. Preserving the multifractal properties of the distribution, we explore three mutually exclusive cases for the mass dependence of $\xi(\alpha, M)$.

(A) Constant width, $\xi(\alpha, M) = A(\alpha)$. A constant width corresponds to the possibility that both the average location of the α sites and the width of the growth zone are not mass dependent, implying that both length scales are proportional to the cluster radius R.

(B) "Strong localization," $\xi(\alpha, M) = A(\alpha)M^{-y}$, $y > 0$, corresponds to a fast decrease of the width of the spatial distribution of the α sites. Asymptotically, the α sites are located at the same distance $x(\alpha)$ from the cluster seed.

(C) "Weak localization," $\xi(\alpha, M) = A(\alpha)/\sqrt{\ln M}$, where the width still tends to zero, but in a logarithmic fashion with intriguing implications for the scaling behavior of $P(x, M)$ and $\rho_A(x, M)$.

A. Constant width: $\xi(\alpha, M) = A(\alpha)$

Substituting relation (11) into (8), we obtain for the Plischke-Rácz probability

$$P(x, M) = \int d\alpha \frac{M^{\nu f(\alpha)} M^{-\nu\alpha}}{\sqrt{2\pi A^2(\alpha)}} \exp\left[-\frac{[x - \bar{x}(\alpha)]^2}{2A^2(\alpha)}\right]. \tag{12}$$

Performing a steepest-descent analysis of (12), we now calculate the value α^* of α at which the integrand is maximal. In the $M \to \infty$ limit, the resulting condition for α^* is

$$\frac{d}{d\alpha} f(\alpha)|_{\alpha^*} = 1. \tag{13}$$

The value of α^* which satisfies Eq. (13) is known to be unity [33], moreover, for $\alpha = 1$ we have $f(\alpha) = 1$. Thus, in case (A), $P(x, M)$ is M independent and has Gaussian shape with constant width $\xi = A(1)$, i.e.,

$$P(x, M) \sim \frac{1}{\sqrt{2\pi A^2(1)}} \exp\left[-\frac{[x - \bar{x}(1)]^2}{2A^2(1)}\right]. \tag{14}$$

Equation (14) does not explicitly depend on M and thus $P(x, M)$ obeys standard scaling.

We perform a similar analysis to evaluate the expres-

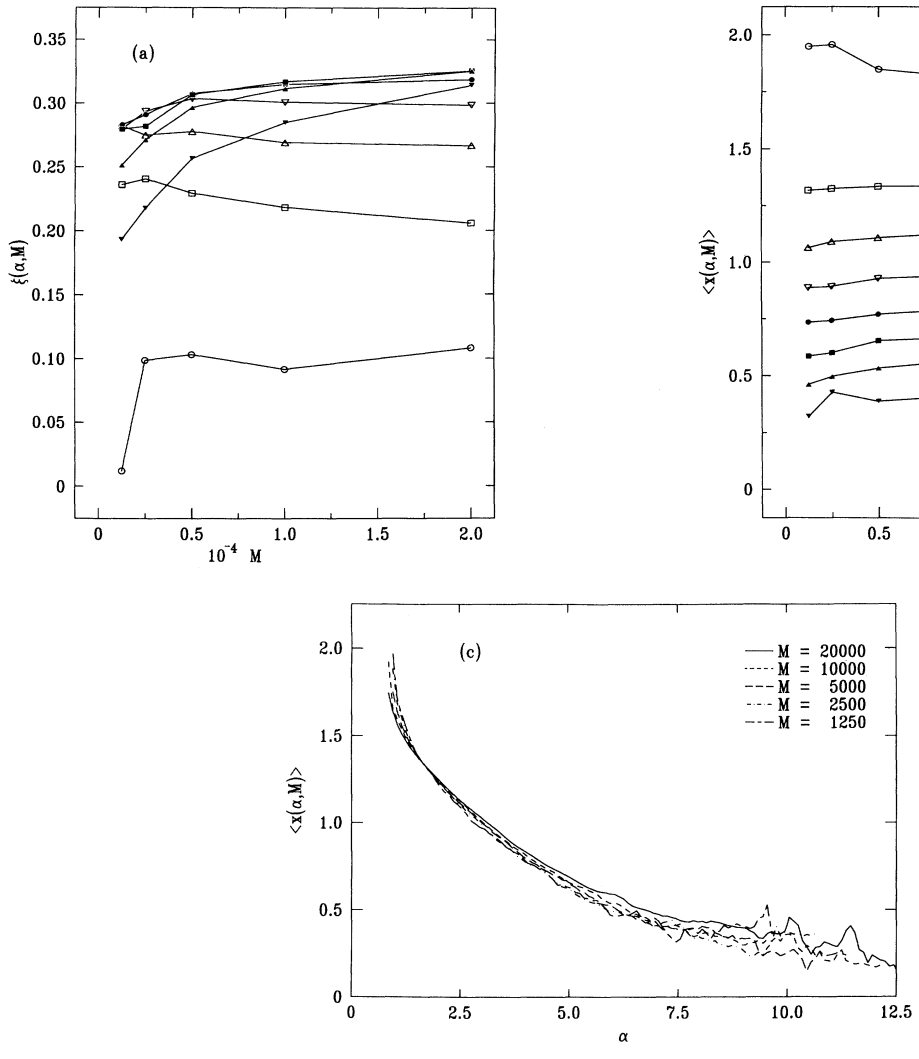

FIG. 6. (a) The width $\xi(\alpha, M)$ and (b) the mean position $\langle x(\alpha, M)\rangle$ vs M for several values of α. Different symbols denote different α values, 0.68 (○), 1.36 (□), 2.04 (△), 2.72 (▽), 3.40 (•), 4.08 (■), 4.76 (▲), and 5.95 (▼). The data are averaged over 18 off-lattice DLA clusters. In (c) $\langle x(\alpha, M)\rangle$ is plotted as a function of α. Here, different line styles correspond to different cluster masses (see legend).

sion (9b) for the density profile of the cluster,

$$\rho_A(x,M) \sim \int d\alpha \frac{M^{\nu f(\alpha)}}{\sqrt{2\pi A^2(\alpha)}} \exp\left[-\frac{[x-\bar{x}(\alpha)]^2}{2A^2(\alpha)}\right]. \quad (15)$$

Here, the condition for the saddle-point value α^* in the limit of large M becomes

$$\frac{d}{d\alpha} f(\alpha)|_{\alpha^*} = 0. \quad (16)$$

The maximum $f(\alpha^*)$ has the value $f(\alpha^*) = 1/\nu$, so that the density can be written as

$$\rho_A(x,M) \sim \frac{M}{\sqrt{2\pi A^2(\alpha^*)}} \exp\left[-\frac{[x-\bar{x}(\alpha^*)]^2}{2A^2(\alpha^*)}\right]. \quad (17)$$

Formally, Eq. (17) can be cast into the form of Eq. (6),

$$\rho_A(x,M) \sim R^{1/\nu} \frac{r^{1/\nu}}{r^{1/\nu}} \exp\left[-\frac{[x-\bar{x}(\alpha^*)]^2}{2A^2(\alpha^*)}\right] = r^{1/\nu} C_\rho(x). \quad (18)$$

Note that in case (A) the exponent of r is independent of x and thus also $\rho_A(x,M)$ obeys standard scaling.

It is instructive to note the meaning of the values α^* from Eqs. (13) and (16) in the multifractal spectrum. The probability to grow at a site with a specific value of α is maximal when the product of growth probability and number of sites with this probability, and thus $f(\alpha) - \alpha$, is maximal. As can be seen by differentiating with respect to α this condition is equivalent to relation (13), from which results the dominant value α^* that controls the $P(x,M)$ integral (12). In contrast, the mass distribution $\rho_A(x,M)$ (15) in the cluster is controlled by the α value corresponding to the maximum of $f(\alpha)$, which is the fractal dimension of the set comprising the "majority" of growth sites.

However, the simple possibility that the width $\xi(\alpha,M)$ of $N(\alpha,x,M)$ is independent of M appears questionable. First, a recent calculation [34] indicates that the width of $P(x,M)$ decreases with M. Second, simulation results for off-lattice DLA clusters with M up to 5×10^7 [29] are consistent with the multiscaling relation (6) for $\rho_A(x,M)$ which precludes an M independent width $\xi(\alpha,M)$.

B. Strong localization: $\xi(\alpha,M) = A(\alpha)M^{-y}$

The implications for case (B), $\xi(\alpha,M) = A(\alpha)M^{-y}$, are quite different from case (A). Now, the analog of Eq. (12) for the Plischke-Rácz probability becomes

$$P(x,M) = \int d\alpha \frac{M^{\nu f(\alpha)-\nu\alpha}}{\sqrt{2\pi A^2(\alpha) M^{-2y}}} \times \exp\left[-M^{2y}\frac{[x-\bar{x}(\alpha)]^2}{2A^2(\alpha)}\right]. \quad (19)$$

For sufficiently large M, the Gaussian function in the integrand tends to a δ function centered at x,

$$x = \bar{x}(\alpha). \quad (20)$$

Given an annulus x, there is only one value of $\alpha = \alpha(x)$ given by the inverse function of $\bar{x}(\alpha)$ — the monotonicity of $\bar{x}(\alpha)$ guarantees the existence of $\alpha(x)$ (cf. Sec. III and Fig. 5).

Using (20), we can compare $P(x,M)$, Eq. (19), to the multiscaling form (4) and find that

$$\phi(x) = -\nu f(\alpha(x)) + \nu\alpha(x). \quad (21)$$

Thus, in contrast to case (A), case (B) results in multiscaling.

In the same fashion, from (9a) and (11) we can demonstrate multiscaling for the density profile of the cluster. Again the Gaussian function in (11) tends to a δ function centered at $x = \bar{x}(\alpha)$ and thus (20) also determines $\alpha(x)$ for the density profile. The resulting density profile $\rho_A(x,M)$ is

$$\rho_A(x,M) \sim M^{\nu f(\alpha)} \sim r^{f(\alpha(x))} C_\rho(x), \quad (22)$$

and displays multiscaling as in Eq. (6) with

$$D(x) = f(\alpha(x)), \quad (23)$$

in agreement with the result of Ref. [27].

The results (21) and (22) are not altogether surprising. In fact, the distribution $N(\alpha,x,M)$ for fixed α tends to a δ function as $M \to \infty$. In this limit, almost all the sites with a specific α value are located at distance $\bar{x}(\alpha)$ from the cluster seed — such that we refer to case (ii) as "strong localization." Vice versa, a specific location x singles out an α value $\alpha(x)$. From $f(\alpha)$ we then obtain the fractal dimension of the set of these $\alpha(x)$ sites. Equation (22) can now be understood just as the usual relationship between mass and extension of a fractal object and, similarly, $M^{-\phi(x)}$, which describes the probability of deposition at x, is just the product of the growth probability $M^{-\nu\alpha(x)}$ at x and the multiplicity of the growth sites at x, $M^{\nu f(\alpha(x))}$.

In the case of strong localization it is particularly simple to obtain an understanding of the relationship between cluster structure and the distribution of growth probabilities. The large α part of $f(\alpha)$ reflects the properties of the frozen region (small x) of the cluster, where the p_i are so small that effectively no further growth will occur. One expects that the mass distribution in the frozen region is characterized by the fractal dimension of DLA. This assumption is supported by the results of Refs. [28,29,34,35]. However, since $\alpha(x)$ is not constant for small x, and if our assumption (11) for the form of the joint distribution function $N(\alpha,x,M)$ is still valid, then $f(\alpha)$ has to be *independent of* α for large α. In fact, the phenomenon of a "phase transition" [36,37] in DLA is consistent with such a behavior of $f(\alpha)$ [22].

C. Weak localization: $\xi(\alpha,M) = A(\alpha)/\sqrt{\ln M}$

For case (C), $\xi(\alpha,M) = A(\alpha)\sqrt{\ln M}$. The exponential in the integrands of (12) and (19) turns into a power law

$$P(x,M)=\int d\alpha\sqrt{\frac{\ln M}{2\pi A^2(\alpha)}}M^{\nu f(\alpha)-\nu\alpha-[x-\bar{x}(\alpha)]^2/2A^2(\alpha)}. \tag{24}$$

Given a value x, a steepest-descent analysis of this integral yields

$$\frac{\partial}{\partial\alpha}\left(\nu f(\alpha)-\frac{[x-\bar{x}(\alpha)]^2}{2A^2(\alpha)}\right)\Bigg|_{\alpha^*}=\nu, \tag{25}$$

as condition for the value α^* maximizing the integrand. As we vary x, the changing value α^* defines a function $\alpha_P(x)$ which enables us to write the Plischke-Rácz probability as

$$P(x,M)=C_{\rm PR}(x)M^{-\phi(x)}, \tag{26}$$

where

$$\phi(x)=-\nu f(\alpha_P(x))+\nu\alpha_P(x)+\frac{[x-\bar{x}(\alpha_P(x))]^2}{2A^2(\alpha_P(x))}, \tag{27}$$

and $C_{\rm PR}(x)$ is an amplitude. By comparison of relation (26) to Eq. (4) we see that case (C) like case (B) results in multiscaling, but with a much more complex multiscaling "exponent" $\phi(x)$.

Although the width $\xi(\alpha,M)$ of $N(\alpha,x,M)$ in case (C) still approaches zero for large M, we note that, in contrast to case (B), α^* is no longer "characteristic" for the shell x — in the sense that Eq. (20) no longer holds. Thus, we refer to case (C) as a case of "weak localization."

To analyze $\rho_A(x,M)$, we first write the condition for α^*. In analogy to (25),

$$\frac{\partial}{\partial\alpha}\left(\nu f(\alpha)-\frac{[x-\bar{x}(\alpha)]^2}{2A^2(\alpha)}\right)\Bigg|_{\alpha^*}=0. \tag{28}$$

The α^* values satisfying Eq. (28) define a function $\alpha_\rho(x)$, when x is varied. Unlike the strong localization case (B), $\alpha_\rho(x)$ differs from $\alpha_P(x)$. We can use the function $\alpha_\rho(x)$ and the method developed in Eq. (18) to express $\rho_A(x,M)$ as

$$\rho_A(x,M)=C_\rho(x)r^{D(x)}, \tag{29}$$

where $C_\rho(x)$ is an amplitude and the multiscaling exponent

$$D(x)=f(\alpha_\rho(x))-\frac{[x-\bar{x}(\alpha_\rho(x))]^2}{2\nu A^2(\alpha_\rho(x))}. \tag{30}$$

The numerical data presented in Sec. III are not sufficient to distinguish between cases (A)–(C) for all values of α. However, for the particular value $\alpha=1.36$, for which the statistics is good, we find the data consistent with case (C). In the following section we will provide further support for the multiscaling idea.

In the preceding discussion we have seen that the existence of two different length scales, namely the average location $\bar{x}(\alpha)$ and the width $\xi(\alpha,M)$ in cases (B) and (C) leads to multiscaling for both $P(x,M)$ and $\rho_A(x,M)$. In contrast, we do not find multiscaling in case (A), where only one length scale is present — both $\bar{x}(\alpha)$ and $\xi(\alpha,M)$ are M independent.

V. MULTIFRACTALITY

Another interesting quantity — possibly accessible to experimental measurements — is the scaling behavior of "moments" of $N(\alpha,x,M)$. In this section, we will define a multifractal analysis for the p_i contained in an annulus at distance x in analogy to the multifractal formalism presented, e.g., in Refs. [20,21].

Usually, a multifractal analysis is performed on a set of numbers that are *normalized.* However, the sum of the growth probabilities p_i restricted to an annulus is less than one, since the p_i are normalized with respect to the entire cluster. Here, we will base our analysis on the *unnormalized* set of p_i at a specific distance x from the cluster seed and postpone to Appendix B a discussion of what happens if we use normalized probabilities instead.

Our first step is to define a "partition function"

$$Z(q,x,M)\equiv\int d\alpha\, N(\alpha,x,M)M^{-q\nu\alpha}, \tag{31}$$

where q is an arbitrary real number [30,38]. The function $Z(q,x,M)$ can also be considered the qth "moment" of the distribution $N(\alpha,x,M)$. Second, we define the scaling indices $\tau(q,x)$ as a function of q for different x by

$$\tau(q,x)\equiv-\lim_{M\to\infty}\frac{\ln Z(q,x,M)}{\nu\ln M}. \tag{32}$$

If $\tau(q,x)$ is a linear function of q, then conventional "gap scaling" is obtained, while otherwise we call the measure underlying the "moments" $Z(q,x,M)$ multifractal. It is then convenient to introduce the Legendre transform $f_L(\alpha_L,x)$ of $\tau(q,x)$

$$f_L(\alpha_L,x)\equiv q\alpha_L-\tau(q,x)\quad\text{where }\alpha_L\equiv\frac{\partial}{\partial q}\tau(q,x). \tag{33}$$

The quantity $f_L(\alpha_L)$ can be interpreted as the fractal dimension of the set of points characterized by α_L [20] in the annulus x. We analyze the scaling behavior of the moments by performing a steepest-descent analysis of (31). Substituting $N(\alpha,x,M)$ in its analytical form (11) into Eq. (31) yields

$$Z(q,x,M)=\int d\alpha\frac{M^{\nu f(\alpha)-\nu q\alpha}}{\sqrt{2\pi\xi^2(\alpha,M)}}\exp\left[-\frac{[x-\bar{x}(\alpha)]^2}{2\xi^2(\alpha,M)}\right]. \tag{34}$$

As in Sec. IV we will now discuss the consequences of different asymptotic behavior of the width of the growth zone of the cluster.

A. Constant width: $\xi(\alpha,M)=A(\alpha)$

For the case of constant width (cf. Sec. IV A), we find that the dominant contribution to the integral (34) arises

at a value $\alpha^* = \alpha^*(1)$ given by

$$\frac{d}{d\alpha} f(\alpha)|_{\alpha^*} = q. \tag{35}$$

From Eq. (35), we can anticipate the result

$$f_L(\alpha_L, x) = f(\alpha_L), \tag{36}$$

which we obtain after consideration of Eqs. (32) and (33). Equation (36) states that *for case (A) the full, unaltered multifractal spectrum is found in all annuli x.* Thus, given the validity of Eq. (11), a constant width of the growth zone can only be maintained, if sites with both low and high growth probabilities are distributed evenly in the cluster [39].

However, due to the the screening of the interior regions of the cluster, the growth probabilities for small x are significantly smaller than at the exposed sites on the exterior of the cluster. These smaller probabilities result in a shift of the distributions $N(\alpha, x, M)$ to larger values of α for small x. Thus, the multifractal spectrum $f_L(\alpha_L)$ differs for different x (cf. [38] for the 3D case), in contrast to the result (36) above.

B. Strong localization: $\xi(\alpha, M) = A(\alpha) M^{-y}$

For the strong localization case (Sec. IV B), the Gaussian term in (34) tends to a δ function localized at x given by Eq. (20) whose inversion gives $\alpha = \alpha(x)$. Now, we use for $Z(q, x, M)$ in Eq. (32) the value of the integrand in (31) at $\alpha = \alpha(x)$. The resulting scaling indices $\tau(q, x)$,

$$\tau(q, x) = q\alpha(x) - f(\alpha(x)), \tag{37}$$

are linearly dependent on q for fixed x. Thus, *in case (B) gap scaling of the moments $Z(q, x, M)$ results.* The $f_L(\alpha_L)$ corresponding to (37) is the point [$\alpha_L = \alpha(x)$; $f_L = f(\alpha(x))$].

The absence of multifractality in a given annulus x in case (B) is not surprising, since the strong localization of α sites implies a very narrow spread of α values within a specific shell x. Narrow distributions, however, typically display gap scaling of their moments.

C. Weak localization: $\xi(\alpha, M) = A(\alpha)/\sqrt{\ln M}$

Again, the weak-localization case is quite different. The value α^* maximizing the integrand of (31) is given by

$$\frac{\partial}{\partial \alpha} \left(\nu f(\alpha) - \frac{[x - \bar{x}(\alpha)]^2}{2A^2(\alpha)} \right) \Bigg|_{\alpha^*} = \nu q. \tag{38}$$

In contrast to Eq. (35), where the solution depends on q only, here α^* is a function of both q and x, and we write $\alpha^* = \alpha_q(x)$. From Eq. (32), we obtain

$$\tau(q, x) = \nu f(\alpha_q(x)) - \nu \alpha_q(x) q - \frac{[x - \bar{x}(\alpha_q(x))]^2}{2A^2(\alpha_q(x))}. \tag{39}$$

In (39) $\tau(q, x)$ is a nonlinear function of both q and x, so that its Legendre transform (33) depends on x. Thus, *in case (C), the multifractal spectrum $f_L(\alpha_L, x)$ is a function of the location of the annulus x.* In contrast to case (B), the width $\xi(\alpha, M)$ approaches zero so slow that the multifractality of case (A) is not destroyed as in case (B), but altered in its character. In fact, the x dependence of the multifractal spectrum $f_L(\alpha_L, x)$ is the hallmark of multiscaling as encountered for $P(x, M)$ and $\rho_A(x, M)$ in case (C), Sec. IV.

In Fig. 7 we display $\tau(q, x)$ for different values of x as a function of q [35].

For large $|q|$ the function $\tau(q, x)$ tends to straight lines with different slopes. The definitions (31) and (32) show that for $q < 0$ the slope is determined by the mass dependence of the smallest growth probability $p_{\min}(x)$ within the annulus x and for $q > 0$ by the mass dependence of the largest growth probability $p_{\max}(x)$, respectively. Especially in the region $0 < q < 1$, we observe a pronounced curvature of $\tau(q, x)$. Since the strong-localization case predicts a linear behavior of $\tau(q, x)$ over the entire range of q values, we conclude that our findings disfavor strong localization.

Moreover, we see that $\tau(q, x)$ displays variation with the parameter x. If x becomes smaller, both $p_{\min}(x)$ and $p_{\max}(x)$ as functions of the cluster mass decay faster, because the interior frozen regions of the cluster are screened stronger. Thus, the two asymptotic slopes (for $q \to \pm\infty$) of $\tau(q, x)$ increase. For example, for any given q, $\tau(q, x = 1.9)$ has everywhere a slope less than $\tau(q, x = 0.7)$. As a consequence, also the Legendre trans-

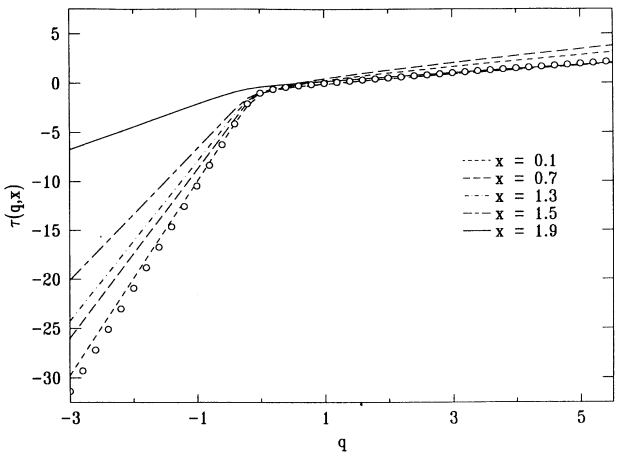

FIG. 7. Dependence on q of $\tau(q, x)$ for different values of x. Here, $\tau(q, x)$ was determined by fitting a straight line through the three data points corresponding to $M = 5000$, 10 000, and 20 000 in a plot of $\ln Z(q, x, M)$ vs $\ln M$ averaged over 18 DLA clusters. Different line styles denote the different x values (legend). For comparison, we plot the $\tau(q)$ resulting from an analysis of the growth probabilities of the entire cluster (○). Since 2D DLA displays a phase transition [40,41], $\tau(q, x)$ for negative q can only be considered an "effective" exponent which will display larger and larger slopes as $M \to \infty$.

TABLE I. Summary of multifractal and multiscaling features arising in cases (A), (B), and (C).

	$\rho_A(x,M)$	$P(x,M)$	$N(\alpha,x,M)$	
	Multiscaling	Multiscaling	Multiscaling	Multifractal
(A) $\xi = A(\alpha)$	no	no	no	yes
(B) $\xi = A(\alpha)/M^y$	yes	yes	yes	no
(C) $\xi = A(\alpha)/\sqrt{\ln M}$	yes	yes	yes	yes

forms of $\tau(q,x)$ are x dependent. This finding is consistent with the weak localization case (C). However, due to the comparatively small clusters that we have analyzed, we cannot exclude cases (A) or (B).

In Fig. 7 we see that $\tau(q,x)$ only starts to change appreciably for quite large x values around $x = 1.5$. A similar phenomenon is observed in the numerical multiscaling analysis of the annular density of the cluster. There, the function $D(x)$ is approximately constant $= 1/\nu$ up to x values of similar magnitude before $D(x)$ drops to zero over a comparatively small range.

For 3D off-lattice DLA, the multifractal properties of the growth probabilities $\{p_i\}$ in an annulus were calculated in [38]. Although no statement about $N(\alpha,x,M)$ for 3D DLA was made, the results display qualitatively the behavior predicted above in the cases (A) and (C) for 2D DLA.

VI. CONCLUSION

We have discussed different possibilities for the analytical form of the joint distribution function $N(\alpha,x,M)$. For cases (B) and (C), where two different length scales enter into $N(\alpha,x,M)$, we find multiscaling behavior of the Plischke-Rácz probability $P(x,M)$ and the density profile $\rho_A(x,M)$ of DLA clusters. Moreover, we find that the scaling behavior of the moments of the growth probability distribution constrained to an annulus x is different in all cases. For (A) and (C), we encounter multifractality, which in case (C) bears an additional feature typical for multiscaling: the x dependence of a scaling "exponent." Our data and previous work are consistent with case (C), although further numerical work to clarify the rich scaling properties of $N(\alpha,x,M)$ is clearly desirable.

Our results for all the different cases discussed above are summarized in Table I.

ACKNOWLEDGMENTS

We wish to thank P. Ossadnik for helpful interactions and comments on the manuscript, and the NSF for financial support. One of the authors (J.L.) thanks the Center for Theoretical Physics at Seoul National University for financial support and hospitality.

APPENDIX A: SPATIAL DISTRIBUTION OF DEAD AND ALIVE PERIMETER SITES

In this appendix, we discuss the properties of the distribution of dead perimeter sites [19]. These sites with growth probability exactly equal to zero result because specific configurations of cluster sites enclose perimeter sites in such a way that they can no longer be reached from the exterior of the DLA cluster. If dead sites are predominantly formed due to specific *local* configurations, then the fraction of perimeter sites that are dead will not change as the cluster grows [19]. Moreover, the spatial distribution of dead sites is then proportional to the distribution of alive sites, i.e.,

$$\rho_A^{(d)}(x,M) \sim \rho_A^{(a)}(x,M) \sim \rho_A(x,M). \tag{A1}$$

On the other hand, if the dead sites were found mainly near the region of small p_i, then $\rho_A^{(d)}(x,M)$ would be shifted towards the center of the cluster. In Fig. 3, we notice that the shape of both distributions looks almost identical. The similarity in form is an evidence favorable to the above-stated "local configuration argument" and shows that the dead sites are uniformly distributed over the cluster.

The simplest local configuration producing a dead site is the L configuration shown in Fig. 1(a). In general, also more complicated configurations will contribute [Figs. 1(b)–(e)]. A coarse graining over the scale of lowest-order configurations of this kind is necessary to see that the densities of dead and alive perimeter sites are proportional. Reference [19] finds a value (0.365 ± 0.010) for the ratio of the number of dead perimeter sites to the total number of perimeter sites for 2D square-lattice DLA.

APPENDIX B: CONSEQUENCES OF NORMALIZATION FOR THE MULTIFRACTAL ANALYSIS

Here, we will briefly explore the consequences of normalizing the growth probabilities p_i within an annulus x prior to performing the multifractal analysis suggested in Sec. V. We determine an x- and M-dependent normalization factor $\mathcal{N}(x,M)$ to multiply each p_i, such that the sum over the growth probabilities for fixed x equals 1. The normalization procedure alters the value of α associated with each p_i to

$$\tilde{\alpha}_i = \ln p_i / \ln R - \ln \mathcal{N}(x,M)/\ln R. \tag{B1}$$

Now, the distribution of the $\tilde{\alpha}$ is $\tilde{N}(\tilde{\alpha},x,M)$, which is related to $N(\alpha,x,M)$ by

$$\tilde{N}(\tilde{\alpha},x,M) = N[\alpha - \ln \mathcal{N}(x,M)/\ln R, x, M]. \tag{B2}$$

In analogy to Eq. (31) we denote the qth moment of $\tilde{N}(\tilde{\alpha}, x, M)$ by $\tilde{Z}(q, x, M)$, i.e.,

$$\tilde{Z}(q,x,M) \equiv \int d\tilde{\alpha}\, \tilde{N}(\tilde{\alpha},x,M) M^{-q\nu\tilde{\alpha}} \tag{B3}$$

$$= \frac{1}{[\mathcal{N}(x,M)]^q} \int d\alpha\, N(\alpha,x,M) M^{-q\nu\alpha} \tag{B4}$$

$$= \frac{1}{[\mathcal{N}(x,M)]^q} Z(q,x,M). \tag{B5}$$

From the normalization we know that the first moment of $\tilde{N}(\tilde{\alpha}, x, M)$ is equal to 1. It follows that $\mathcal{N}(x, M) = Z(1, x, M)$.

We continue along the lines in Sec. V and define the equivalent $\tilde{\tau}(q, x)$ to $\tau(q, x)$,

$$\tilde{\tau}(q,x) \equiv -\lim_{R\to\infty} \frac{\partial \ln \tilde{Z}(q,x,M)}{\partial \ln R} \tag{B6}$$

$$= \tau(q,x) + q \lim_{R\to\infty} \frac{\partial \ln \mathcal{N}(x,M)}{\partial \ln R}. \tag{B7}$$

If the normalization constant $\mathcal{N}(x, M)$ displays power-law scaling with the cluster size R, then $\tilde{\tau}(q, x)$ and $\tau(q, x)$ differ only by a linear function. How does this difference affect the Legendre transform of $\tilde{\tau}(q, x)$ when we compare it to the transform of $\tau(q, x)$, which is defined in Eq. (33)? First, we calculate the slope $\tilde{\alpha}_L$ of $\tau(q, x)$,

$$\tilde{\alpha}_L = \frac{\partial \tilde{\tau}(q,x)}{\partial q} = \alpha_L + \lim_{R\to\infty} \frac{\partial \ln \mathcal{N}(x,M)}{\partial \ln R}. \tag{B8}$$

Since $\mathcal{N}(x, M)$ is always less than one, we see that $\tilde{\alpha}_L$ is merely α_L shifted by a constant to smaller values. Second, Legendre transforming $\tilde{\tau}(q, x)$ yields

$$\tilde{f}_L(\tilde{\alpha}_L) = q\tilde{\alpha}_L - \tilde{\tau}(q,x) \tag{B9}$$

$$= q\alpha + q \lim_{R\to\infty} \frac{\partial \ln \mathcal{N}(x,M)}{\partial \ln R} \tag{B10}$$

$$-\tau(q,x) - q \lim_{R\to\infty} \frac{\partial \ln \mathcal{N}(x,M)}{\partial \ln R}$$

$$= q\alpha - \tau(q,x) = f_L(\alpha_L). \tag{B11}$$

Thus, we retain the functional form of the Legendre transform $f_L(\alpha_L)$ of $\tau(q, x)$ and the only difference to $\tilde{f}(\tilde{\alpha}_L)$ is that the latter is shifted towards smaller values of α.

For example, if we use the formalism presented in this appendix to calculate the $\tilde{f}_L(\tilde{\alpha}_L)$ for the strong-localization case (cf. Sec. V B), we find that

$$\tilde{f}_L(\tilde{\alpha}_L) = f_L, \quad \tilde{\alpha} = f_L, \tag{B12}$$

where f_L denotes the constant value of $f_L(\alpha(x))$ for a given x. In order to interpret the result (B12), consider the normalization condition $\sum_i \tilde{p}_i(x) = 1$ within an annulus. In the strong-localization case, the annulus x is characterized by only one α. Thus, the product $M^{-\nu\tilde{\alpha}} M^{\nu f(\tilde{\alpha})}$ must be constant, leading to $\tilde{\alpha} = f_L$.

[1] T. A. Witten and L. Sander, Phys. Rev. Lett. **47**, 1400 (1981).
[2] L. A. Turkevich and H. Scher, Phys. Rev. Lett. **55**, 1026 (1985).
[3] R. C. Ball, R. M. Brady, G. Rossi, and B. R. Thompson, Phys. Rev. Lett. **55**, 1406 (1985).
[4] A. Coniglio, in *On Growth and Form: Fractal and Non-Fractal Patterns in Physics*, edited by H. E. Stanley and N. Ostrowsky (Nijhoff, Dordrecht, 1985), p. 101.
[5] G. Parisi and Y. C. Zhang, J. Stat. Phys. **41**, 1 (1985).
[6] Y. Hayakawa, S. Sato, and M. Matsushita, Phys. Rev. A **36**, 1963 (1987).
[7] T. C. Halsey, Phys. Rev. Lett. **59**, 2067 (1987).
[8] L. Pietronero, A. Erzan, and C. J. G. Evertsz, Phys. Rev. Lett. **61**, 861 (1988).
[9] P. Meakin, in *Phase Transitions and Critical Phenomena*, edited by C. Domb and J. L. Lebowitz (Academic, Orlando, 1988), Vol. 12.
[10] J. Feder, *Fractals* (Pergamon, New York, 1988).
[11] *Random Fluctuations and Pattern Growth: Experiments and Models*, edited by H. E. Stanley and N. Ostrowsky (Kluwer Academic, Dordrecht, 1988).
[12] *Fractals: Physical Origin and Properties*, edited by L. Pietronero (Plenum, London, 1990).
[13] *Fractals and Disordered Systems*, edited by A. Bunde and S. Havlin (Springer, Berlin, 1991).
[14] T. Vicsek, *Fractal Growth Phenomena*, 2nd ed. (World Scientific, Singapore, 1992).
[15] P. Meakin, H. E. Stanley, A. Coniglio, and T. A. Witten, Phys. Rev. A **32**, 2364 (1985).
[16] P. Meakin, A. Coniglio, H. E. Stanley, and T. A. Witten, Phys. Rev. A **34**, 3325 (1986).
[17] T. C. Halsey, P. Meakin, and I. Procaccia, Phys. Rev. Lett. **56**, 854 (1986).
[18] C. Amitrano, A. Coniglio, and F. di Liberto, Phys. Rev. Lett. **57**, 1016 (1986).
[19] C. Amitrano, P. Meakin, and H. E. Stanley, Phys. Rev. A **40**, 1713 (1989).
[20] B. B. Mandelbrot, J. Fluid Mech. **62**, 331 (1974); H. G. E. Hentschel and I. Procaccia, Physica D **8**, 435 (1983); U. Frisch and G. Parisi, in *Turbulence and Predictability in Geophysical Fluid Dynamics and Climate Dynamics*, edited by M. Ghil, R. Benzi, and G. Parisi (North-Holland, New York, 1985), p. 84; T. C. Halsey, M. H. Jensen, L. P. Kadanoff, I. Procaccia, and B. I. Shraiman, Phys. Rev. A **33**, 1141 (1986).
[21] H. E. Stanley and P. Meakin, Nature **335**, 405 (1988).
[22] B. B. Mandelbrot, C. J. G. Evertsz, and Y. Hayakawa, Phys. Rev. A **42**, 4528 (1990).
[23] B. B. Mandelbrot and C. J. G. Evertsz, Physica A **177**, 386 (1991).
[24] S. Schwarzer, J. Lee, S. Havlin, H. E. Stanley, and P. Meakin, Phys. Rev. A **43**, 1134 (1991).
[25] M. Plischke and Z. Rácz, Phys. Rev. Lett. **53**, 415 (1984).
[26] P. Meakin and L. M. Sander, Phys. Rev. Lett. **54**, 2053 (1985).

[27] A. Coniglio and M. Zannetti, Physica A **163**, 325 (1990).
[28] C. Amitrano, A. Coniglio, P. Meakin, and M. Zanetti, Phys. Rev. B **44**, 4974 (1991).
[29] P. Ossadnik, Physica A **195**, 319 (1993).
[30] In the context of turbulence a connection between a sort of multiscaling and multifractality has been discussed by M. H. Jensen, G. Paladin, and A. Vulpiani, Phys. Rev. Lett. **67**, 208 (1991).
[31] P. Meakin, I. Majid, S. Havlin, and H. E. Stanley, J. Phys. A **17**, L975 (1984).
[32] A more general form for $N(\alpha, x, M)$ would include a power-law function of x multiplying the pure Gaussian behavior [34]. However, such an x-dependent term would not invalidate the discussion in the subsequent sections and so we adhere to the Gaussian form for the purposes of this paper.
[33] N. G. Makarov, Proc. London Math. Soc. **51**, 369 (1985).
[34] P. Ossadnik and J. Lee, J. Phys. A (to be published).
[35] P. Ossadnik, Physica A **176**, 454 (1991).
[36] Since the small-growth probabilites in 2D DLA vanish faster than any power of M, DLA displays a phase transition in its multifractal spectrum. This phase transition manifests itself in increasing slopes of $\tau(q, x)$ for negative q, when $\tau(q, x)$ is estimated from clusters with increasingly larger masses M. We expect it to occur for all x for which $\tau(q, x)$ is defined, since Ref. [39] has demonstrated that the small growth probabilties are spatially distributed over the entire cluster.
[37] J. Lee, P. Alstrøm, and H. E. Stanley, Phys. Rev. A **39**, 6545 (1989).
[38] For 3D off-lattice DLA, the multifractal spectrum in a shell around the cluster seed was investigated in S. Schwarzer, S. Havlin, and H. E. Stanley, Physica A **191**, 117 (1992); S. Schwarzer, M. Wolf, S. Havlin, P. Meakin, and H. E. Stanley, Phys. Rev. A **46**, R3016 (1992).
[39] B. B. Mandelbrot and C. J. G. Evertsz, Nature **348**, 143 (1990).
[40] J. Lee and H. E. Stanley, Phys. Rev. Lett. **61**, 2945 (1988); S. Schwarzer, J. Lee, A. Bunde, H. E. Ronan, S. Havlin, and H. E. Stanley, *ibid.* **65**, 603 (1990).
[41] R. Blumenfeld and A. Aharony, Phys. Rev. Lett. **62**, 2977 (1989).